



# A $3_{10}$ -helix single turn enforced by crosslinking of lysines with 1,1'-ferrocenedicarboxylic acid

Timothy P. Curran \*, Emma L. Handy

Department of Chemistry, Trinity College, Hartford, CT 06106-3100, USA

## ARTICLE INFO

### Article history:

Received 2 September 2008

Received in revised form 22 November 2008

Accepted 24 November 2008

Available online 6 December 2008

### Keywords:

Ferrocene

Peptide

Conformation

Bioorganometallic

## ABSTRACT

Prior work has shown that covalently linking the side chains of amino acids in the *i* and *i*+3 and *i* and *i*+4 positions in a peptide will enforce a helical conformation. In this work the ability of an organometallic entity to enforce a helical conformation in a peptide was explored. The tetrapeptide Boc-Lys-Ala-Val-Lys-NHCH<sub>3</sub> was prepared, then reacted with 1,1'-ferrocenedicarboxylic acid chloride. Reaction of the lysine side chain amines with the diacid chloride resulted in a metallacyclicpeptide (**1**) in which the two lysines are crosslinked via the ferrocene. The solution conformation of the metallacyclicpeptide (**1**) was studied using CD and NMR spectroscopy. The NMR methods employed were Karplus analysis of coupling constants, chemical shift changes of NH protons and ROESY data. The results show that the metallacyclicpeptide (**1**) adopts a single turn of the  $3_{10}$ -helix conformation.

© 2008 Elsevier B.V. All rights reserved.

## 1. Introduction

Helices are an important structural feature of nearly all known proteins [1]. In addition to defining the overall tertiary structure of a protein, helices also possess distinct and important biochemical functions. This is particularly true with respect to biochemical signalling pathways that are triggered by protein-protein and protein-DNA interactions [2,3]. As an example, the binding of a helical peptide to the protein Bcl-X<sub>L</sub> can induce apoptosis of cancer cells [4–6].

Because protein helices can mediate important biochemical pathways, efforts have been made to excise the helical portion of a protein and use it in place of the whole protein. Unfortunately, in most cases, excision of a helical segment from a larger protein yields a peptide that adopts a random coil conformation [7]; from these results it has been concluded that constraints imposed by other parts of the protein are needed to maintain the helical shape.

Synthetic chemists have been able to hold short peptides in helical conformations by introducing non-natural constraints [8–11]. These constraints can be located at various places in a peptide chain. In one approach, a constraint that keeps the initial residues of a peptide in a helical conformation can be added to either the N-terminus [12,13] or the C-terminus [14] of the peptide; subsequent amino acids added to the peptide are then positioned so they propagate the helix. In another approach, a constraint can be added by linking the side chains of two amino acid residues. This link can be made using an amide bond [8–11,15], a disulfide [8–11,16], or

metal–ligand interactions [8–11,17,18]. The connection can also be made by bridging the side chains of two amino acids with a covalent spacer [8–11,19]. Linking the side chains forces the internal portion of the peptide to be helical; those parts of the peptide adjacent to the constraint are then positioned to propagate the helix. In a third approach, the constraint can be made by replacing the intramolecular hydrogen bond with a covalent spacer [5,20]. As with the other approaches, this constraint enforces a helical conformation on a small part of the peptide; amino acid residues outside the constraint are then positioned to extend the helix.

We are interested in developing a helix constraint that is easy to introduce using both solution and solid phase peptide synthesis protocols, and that possesses a unique chromophore. These two properties, which are not present together in the known helix constraints, would allow researchers to quickly generate peptide helices, and then develop UV–Vis spectroscopic methods for analyzing the ability of these synthetic helices to bind to biochemical targets. A constraint employing an organometallic entity would meet these criteria. Herein we report the use of the ferrocene as a side chain constraint that can enforce a helical conformation.

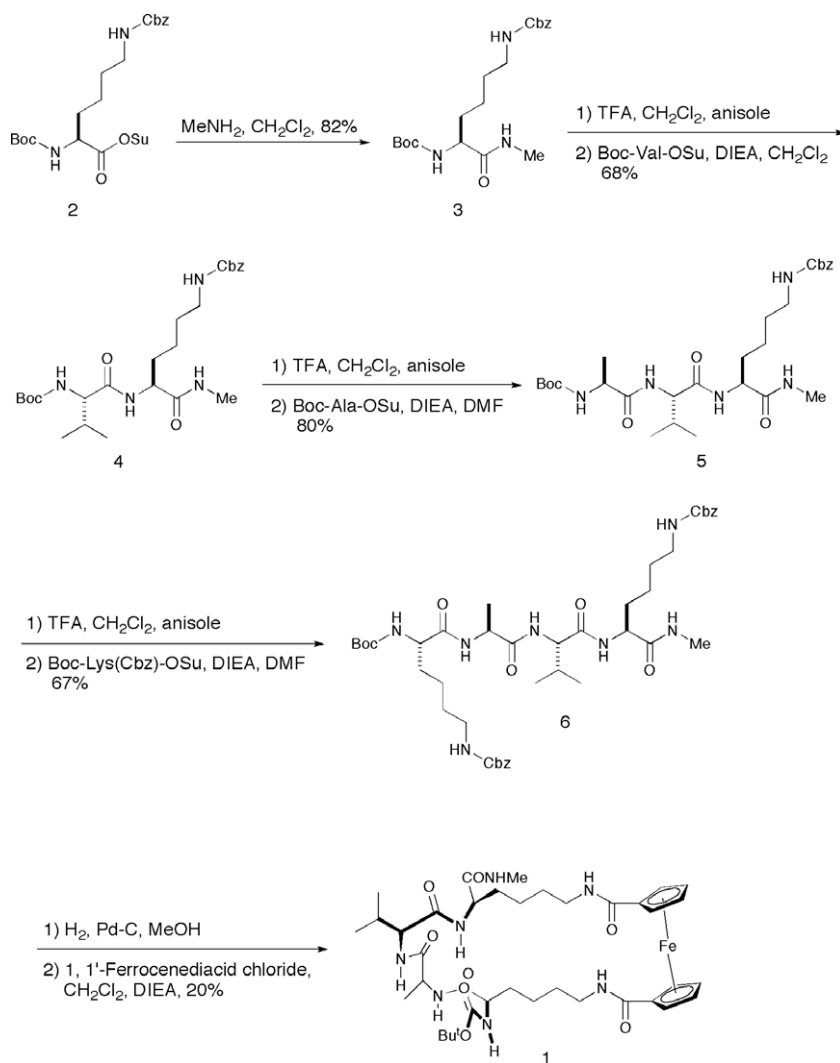
## 2. Results and discussion

### 2.1. Synthesis of **1**

The molecule studied was metallacyclic tetrapeptide (**1**) (Scheme 1), which has lysines at the 1 and 4 positions, and alanine and valine at positions 2 and 3. Lysine was chosen as the crosslinking amino acid because it has a reactive functional group (an amine) and its side chain is long enough to allow for cyclization.

\* Corresponding author.

E-mail address: [timothy.curran@trincoll.edu](mailto:timothy.curran@trincoll.edu) (T.P. Curran).



**Scheme 1.** Synthesis of metallacyclictetrapeptide (**1**).

In **1** the side chain amines of the two lysines are joined to each other via amide bonds made to the two carboxyls from 1,1'-ferrocenediacid. This diacid and its derivatives have been used by other researchers to constrain peptide conformations [21–27]. We hypothesized that the ferrocene crosslink would enforce a helical conformation for the peptide part of **1**. From previous work it is known that helices can be generated by linking amino acid side chains in the 1 and 4 positions [28–31]. Valine and alanine were selected because of their demonstrated tendency to appear in protein helices [1], and because the chemical shifts of their protons were unlikely to overlap with the amide NH protons in NMR spectra.

The synthesis of **1** is outlined in Scheme 1. Commercially available Boc-Lys(Cbz)-OSu (**2**) was reacted with N-methylamine to generate **3**. Removal of the Boc group using TFA, followed by reaction of the resulting amine with Boc-Val-OSu yielded dipeptide **4**. Repetition of the same protocol (deprotection of the Boc group followed by reaction with Boc-Ala-OSu) generated tripeptide **5**. In a similar way the tetrapeptide **6** was produced by Boc group removal and coupling with **2**. In all these reactions the peptide product was isolated using an extraction procedure; no further purification was attempted. The crude products were pure enough (as judged by TLC) that they could be used in the next step of the synthesis.

The ferrocene crosslink was made by removal of the two Cbz groups from **6** using catalytic hydrogenation. The resulting diamine was then reacted with 1,1'-ferrocenediacid chloride [32] (under dilute conditions) to yield **1**. The metallacyclipeptide (**1**) was purified to homogeneity by flash chromatography and characterized by HPLC, <sup>1</sup>H NMR spectroscopy, electrospray ionization mass spectrometry and high-resolution mass spectrometry. Metallacyclipeptide (**1**) is an amorphous, orange solid. Efforts to crystallize **1** have so far been unsuccessful, so an X-ray crystal structure has not been obtained.

## 2.2. Conformational analysis

Both NMR and CD spectroscopy were used to determine the conformation of **1**. With CD spectroscopy, it is well known that helical peptides exhibit spectra in which there are two absorbance minima located at 208 and 222 nm [33]. To see whether **1** adopts a helical conformation, the CD spectrum was obtained in CHCl<sub>3</sub> (Fig. 1). This spectrum closely matches the classical CD spectrum for an  $\alpha$ -helix as it shows two absorbance minima at 201 and 220 nm. The overall appearance of the CD spectrum of **1** indicates that it is helical.

To more firmly establish the helical conformation of **1**, proton assignments were made by analysis of the COSY spectrum of **1** in

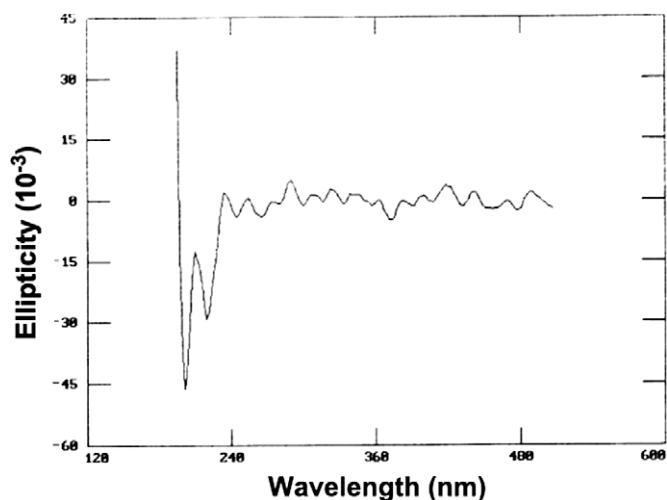


Fig. 1. The CD spectrum of **1** recorded in  $\text{CHCl}_3$ . The spectrum shows two minima at 201 and 220 nm, which indicates that **1** adopts a helical conformation.

Table 1  
Chemical shift,  $J_{\text{NH}-\text{C}\alpha\text{H}}$  and dihedral angle ( $\theta$ ) data for **1** in  $\text{CDCl}_3$ .

NH proton	$\delta$ (ppm)	$J_{\text{NH}-\text{C}\alpha\text{H}}$ (Hz)	$\theta^a$	$\theta^b$
Lys (C-terminus)	7.31	7.5	$-144^\circ$	$-154^\circ$
Val	7.11	6.2	$-137^\circ$	$-113^\circ$
Ala	6.58	3.3	$-120^\circ$	$-153^\circ$
Lys (N-terminus)	5.31	2.8	$-117^\circ$	$-93^\circ$

<sup>a</sup> Dihedral angles for **1** calculated from the measured  $J_{\text{NH}-\text{C}\alpha\text{H}}$  values (see Ref. [36]).

<sup>b</sup> Dihedral angles for **1** obtained from the computer model of **1** displayed in Fig. 1. The computer model was generated using Spartan 04.

$\text{CDCl}_3$ . In this way the NH protons for each individual amino acid in **1** were identified (see Table 1 for selected NH chemical shifts). There is a wide separation of chemical shifts among the different NH protons. These chemical shift differences indicate that each NH is in a distinctly unique environment, as would be expected if **1** adopts a helical conformation [12,13].

Having identified each NH resonance, the  $J_{\text{NH}-\text{C}\alpha\text{H}}$  values for each amide proton were measured (Table 1). For a helical peptide,  $J_{\text{NH}-\text{C}\alpha\text{H}}$  values usually fall in the range between 3 and 5 Hz [34]. As the data shows, the NH from the N-terminal lysine and the NH from the alanine fall in this range. The valine resonance falls just outside this range, while the resonance for the C-terminal lysine is outside this range. The trend is for the  $J_{\text{NH}-\text{C}\alpha\text{H}}$  values to move away from the 3 to 5 Hz range as the peptide progresses from the N-terminus to the C-terminus. Using the Karplus equation, the dihedral angles for the measured coupling constants were calculated, and these values are also given in Table 1 [35].

To gain some insight into the coupling constant data, a model of **1** was constructed using Spartan 04. The calculated dihedral angles from Table 1 were used to set the starting conformations for the NH protons in the model. After this, the resulting structure was minimized. The conformation of **1** that was obtained is shown in Fig. 2. This structure has the peptide in the conformation of a single turn of a  $3_{10}$ -helix [36].

The dihedral angles for each  $\text{NH}-\text{C}\alpha\text{H}$  in the model of **1** were then measured and are reported in Table 1. In general, the computer model produces slightly larger dihedral angles than those calculated from the coupling constants and the Karplus equation. However, the trend in the dihedral angles is the same for the values derived from the Karplus equation and from the energy minimized computer model. In an idealized  $3_{10}$ -helix, the  $\text{NH}-\text{C}\alpha\text{H}$  dihedral

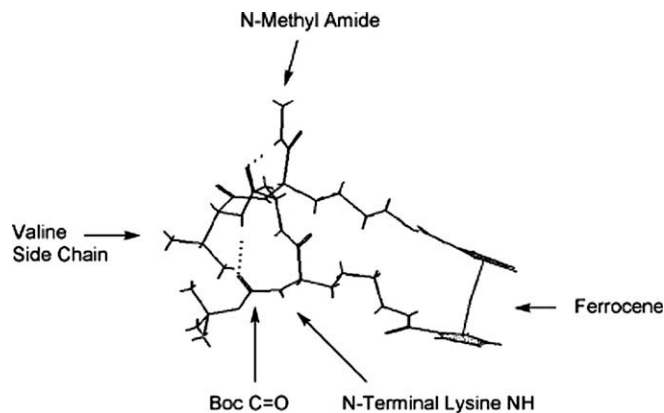


Fig. 2. Molecular model of compound **1**.

angle is  $-120^\circ$  [36]. With both the NMR and modeling data the dihedral angles are within the range of dihedral angles found for  $3_{10}$ -helices seen in protein crystal structures [37].

In order to confirm that **1** adopts a  $3_{10}$ -helix conformation, the ROESY spectrum of **1** was obtained in  $\text{CDCl}_3$ . As noted by many researchers, including Kemp [12,13], Bartlett [14], and Arora [20], a signature of helices is the observation of NOEs between consecutive amide NH protons [ $d_{\text{NN}}(i, i+1)$ ]. The amide NH region portion of the ROESY spectrum of **1** is shown in Fig. 3. The data shows that the NH protons in **1** have crosspeaks with the adjacent NH protons. Thus, the N-terminal lysine NH shows a crosspeak only to the alanine NH. In turn, the alanine NH only shows a crosspeak to the valine NH, and the valine NH only shows a crosspeak to the C-terminal lysine NH, and the C-terminal lysine NH only shows a crosspeak to the N-methyl amide NH. This pattern of ROESY crosspeaks among the amide NH protons in **1** is consistent with the  $3_{10}$ -helix conformation shown in Fig. 2.

In addition to the detection of close contacts between adjacent amide NH protons, helical conformations can also be detected through the observations of NOEs between resonances on amino acid residues brought into close proximity by the twisting of the peptide chain. If **1** assumes the conformation shown in Fig. 2, then the valine residue will be in close proximity to the two end lysine residues. Fig. 4 shows the crosspeaks to the valine methyl resonance in the ROESY spectrum of **1** in  $\text{CDCl}_3$ . These methyl groups show crosspeaks to the valine NH,  $\text{C}\alpha\text{H}$  and  $\text{C}\beta\text{H}$  protons, the NH and  $\text{C}\alpha\text{H}$  protons from the C-terminal lysine, and the  $\text{C}\alpha\text{H}$  proton from the N-terminal lysine. That the valine methyl produces NOEs to both lysine  $\text{C}\alpha\text{H}$  protons can only be true if **1** adopts a  $3_{10}$ -helix conformation.

Further evidence from the ROESY spectrum that supports the conclusion that **1** adopts a  $3_{10}$ -helix conformation comes from analysis of the crosspeaks of the valine  $\text{C}\alpha\text{H}$  protons in the ROESY spectrum of **1**. In addition to showing crosspeaks to the valine methyls,  $\text{C}\beta\text{H}$  and NH protons, the valine  $\text{C}\alpha\text{H}$  also shows crosspeaks to the NH protons from the C-terminal lysine and the N-methylamide. The presence of an NOE between the valine  $\text{C}\alpha\text{H}$  and the N-methylamide NH can only occur if **1** adopts a  $3_{10}$ -helix conformation.

To further confirm that **1** adopts a helical conformation in solution, the  $^1\text{H}$  NMR, COSY and ROESY spectra of **1** was recorded in  $d_6$ -acetone. The ROESY spectrum of **1** in  $d_6$ -acetone showed the same pattern of crosspeaks between the NH protons as was seen in  $\text{CDCl}_3$ , and the coupling constants for the NH protons were of similar magnitudes. Both results show that the conformation of **1** is unchanged in going from  $\text{CDCl}_3$  to  $d_6$ -acetone.

One method that has been successfully used to detect intramolecular hydrogen bonds in peptides is the use of solvent titration

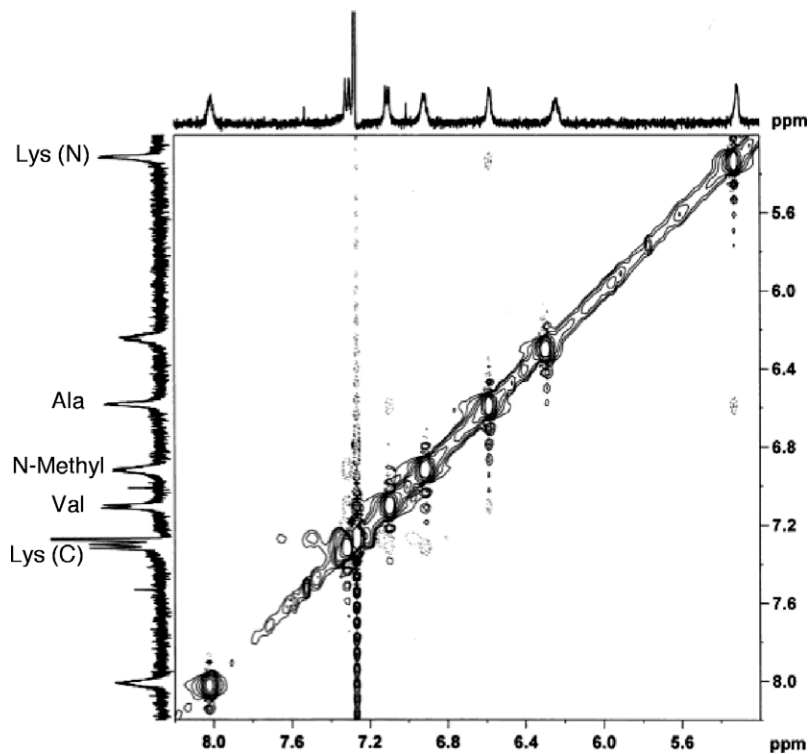


**Fig. 3.** The amide NH region of the ROESY spectrum of **1** in  $\text{CDCl}_3$ . The chemical shifts of the amide NH protons in **1** determined from the COSY spectrum are: N-methyl (6.9 ppm), N-terminal Lys (5.3 ppm), Ala (6.6 ppm), Val (7.1 ppm), C-terminal Lys (7.3 ppm), Lys-ferrocene amides (8.0 and 6.2 ppm). The pattern of crosspeaks here is consistent with a helical conformation for **1**.

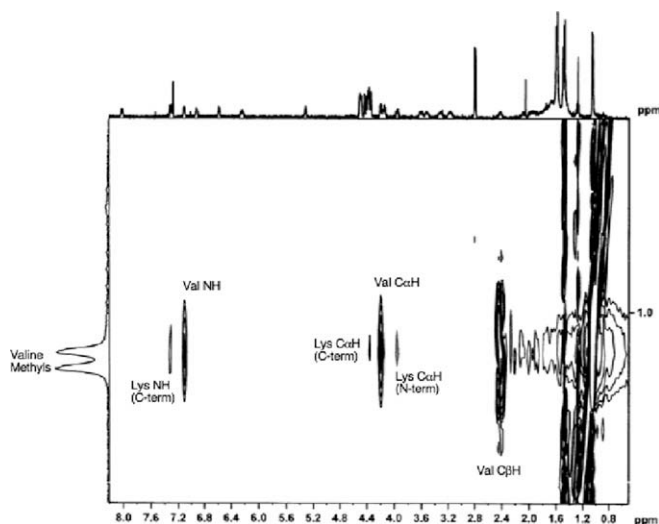


**Fig. 4.** A portion of the ROESY spectrum of **1** in  $\text{CDCl}_3$  showing the crosspeaks to the valine methyl resonances.

[38–43]. Unlike chloroform, acetone is an aggressive hydrogen bond acceptor. Accordingly, the chemical shifts of the NH protons in **1** will differ greatly between chloroform and acetone if they interact with the solvent. If, however, an NH proton in **1** is protected from the solvent by being involved in an intramolecular hydrogen bond, then the chemical shift of that proton will not change much in going from chloroform to acetone. If **1** adopts the  $3_{10}$ -helix conformation shown in Fig. 1, then the mainchain NH protons from the N-terminal lysine and the alanine should show a large chemical shift change from chloroform to acetone, while the mainchain NH protons from the valine, C-terminal lysine

and N-methyl amide should show little or no change in chemical shift as the solvent is changed. In contrast, if **1** adopts an  $\alpha$ -helical conformation, then the mainchain NH protons from the N-terminal lysine, the alanine and the valine should show a large chemical shift change from chloroform to acetone, while only the mainchain NH protons from the C-terminal lysine and the N-methyl amide should show little or no change in chemical shift as the solvent is changed. Thus, the key marker to distinguish an  $\alpha$ -helix from a  $3_{10}$ -helix is the behavior of the valine NH resonance. A large change in its chemical shift would indicate an  $\alpha$ -helical conformation; a small change would indicate a  $3_{10}$ -helical conformation.

Given in Table 2 are the chemical shifts for the NH protons in **1** in both  $\text{CDCl}_3$  and  $d_6$ -acetone. The three NH protons starting from the C-terminus (N-methyl, lysine and valine NH protons) exhibit very small changes in chemical shift (<0.2 ppm) in going from  $\text{CDCl}_3$  to  $d_6$ -acetone. In contrast, the two NH protons starting from the N-terminus (alanine and lysine) exhibit a very large change in chemical shift (>1.3 ppm). This data indicates that the three NH protons starting from the C-terminus, including the valine NH, are involved in intramolecular hydrogen bonds, while the two NH protons starting from the N-terminus are not involved in intramolecular hydrogen bonds. This behavior is consistent with a  $3_{10}$ -helix conformation for **1** as shown in Fig. 2.

**Table 2**  
Chemical shift comparisons for **1** in  $\text{CDCl}_3$  and  $d_6$ -acetone.

NH proton	$\delta$ (ppm) $\text{CDCl}_3$	$\delta$ (ppm) $d_6$ -acetone	$\Delta\delta$ (ppm)
N-Methyl	6.92	7.08	+0.16
Lys (C-terminus)	7.31	7.46	+0.15
Val	7.11	7.31	+0.20
Ala	6.58	8.05	+1.47
Lys (N-terminus)	5.31	6.64	+1.33



The combination of CD,  $J_{\text{NH-C}\alpha\text{H}}$ , ROESY, solvent titration and molecular modeling data for **1** shows that the ferrocene crosslink enforces the conformation of a single turn of a  $3_{10}$ -helix in the tetrapeptide portion of this metallacyclicpeptide. This conclusion is buttressed by results from other researchers which have shown that  $3_{10}$ -helices can be generated by crosslinking the side chains of amino acids in the *i* and *i*+3 positions in a peptide [30,31]. Since it is relatively easy using one of the common 20 amino acids to introduce the ferrocene crosslink, and that the chemical steps to do so are amenable to solid phase peptide synthesis, and that the crosslink gives the peptide a unique and useful chromophore, this new method for generating helices has great potential. Further studies to determine whether a single turn of an  $\alpha$ -helix can be generated and to demonstrate that the helix can be propagated beyond the single turn are underway.

### 3. Experimental

#### 3.1. General procedures

Amino acid derivatives were purchased from ChemImpex International. Anisole and DMF (dimethylformamide) were purchased from Sigma–Aldrich. TFA, DIEA, and THF were purchased from Acros Organics. 1,1'-Ferrocenedicarboxylic acid was purchased from Strem Chemical.  $\text{CDCl}_3$  and  $d_6$ -DMSO were purchased from Cambridge Isotope Labs. Silica gel for flash chromatography was purchased from Silicycle. CD spectra were recorded using a Cary-16/OLIS spectrometer using a 3 mg/mL solution of **1** in  $\text{CHCl}_3$  in a quartz cell (0.100 cm pathlength). NMR spectra were obtained on either a GE Omega 300 MHz instrument or a Bruker AVANCE III 400 MHz instrument. Electrospray mass spectra were obtained on a LCQ APCI/Electrospray LC MS–MS. Samples for ESI mass spectral analysis were dissolved in MeOH (approximately 1 mg/mL) in borosilicate glass test tubes. High-resolution mass spectra were obtained on a JEOL AccuTOF DART mass spectrometer. HPLC analyses were performed on a Finnigan MAT SpectraSystem HPLC using a Vydac C18 peptide column. The gradient used started with 80% TFA (0.1%)/20%  $\text{CH}_3\text{CN}$  and went to 50% TFA (0.1%)/50%  $\text{CH}_3\text{CN}$  in a 6.0 min span. Next, the gradient went from 50% TFA (0.1%)/50%  $\text{CH}_3\text{CN}$  to 0% TFA (0.1%)/100%  $\text{CH}_3\text{CN}$  over the next 6.0 min. The flow rate was 1.0 mL/min. For the final 8.0 min of the analysis the solvent remained at 0% TFA (0.1%)/100%  $\text{CH}_3\text{CN}$ . The UV–Vis detector was set at 410 nm. Peptides **3–6** were isolated as crude products with relatively high purity as judged by TLC. They were not purified; instead they were taken on to the next step in the synthesis as is.

#### 3.2. Preparation of Boc-Lys(Cbz)-NHMe (**3**)

To a solution of 3.100 g (6.492 mmol) of Boc-Lys(Cbz)-OSu (**2**) dissolved in 50 mL  $\text{CH}_2\text{Cl}_2$  was added 10 mL of 2.0 M  $\text{CH}_3\text{NH}_2$  in THF. The resulting solution stirred at 23 °C for 4 h. The solvent was evaporated and the residue that remained was redissolved in 50 mL EtOAc. This solution was washed: 3 × 50 mL 0.1 M HCl, 3 × 50 mL saturated  $\text{NaHCO}_3$ , and 1 × 50 mL brine. The organic layer was dried ( $\text{MgSO}_4$ ), filtered and evaporated to yield 2.079 g (82%) of **3** as a white solid: m.p. 64–66 °C; TLC,  $R_f$  0.45 (EtOAc); ESI-MS M+Na ion calculated for  $\text{C}_{20}\text{H}_{31}\text{N}_3\text{O}_5\text{Na}$ , 416 *m/z*; found, 415.7 *m/z*;  $^1\text{H}$  NMR (400 MHz,  $\text{CDCl}_3$ ) *d* 7.40–7.30 (5H, m), 6.12 (1H, m), 5.11 (3H, m), 4.85 (1H, m), 4.03 (1H, m), 3.20 (2H, m), 2.82 (3H, d, *J* = 4.9 Hz), 2.0–1.3 (6H, m), 1.44 (9H, s).

#### 3.3. Preparation of Boc-Val-Lys(Cbz)-NHMe (**4**)

A solution of 2.079 g (5.290 mmol) of Boc-Lys(Cbz)-NHMe (**3**) in 15 mL  $\text{CH}_2\text{Cl}_2$  and 1.0 mL of anisole was chilled to 5 °C in an ice

water bath. To the chilled solution was added 8.0 mL TFA. The resulting solution stirred for 1.5 h while it slowly warmed to 23 °C. The solvents were evaporated to yield a yellow oil. This oil was dried under high vacuum to remove any last traces of TFA. Next, the oil was redissolved in 15 mL  $\text{CH}_2\text{Cl}_2$ . To this solution was added 1.714 g (5.459 mmol) of Boc-Val-OSu and 22 mL (132 mmol) of DIEA. The resulting solution stirred at 23 °C for 4 h. The solvent was evaporated and the residue that remained was redissolved in 75 mL EtOAc. This solution was washed: 3 × 75 mL 0.1 M HCl, 3 × 75 mL saturated  $\text{NaHCO}_3$ , and 1 × 75 mL brine. The organic layer was dried ( $\text{MgSO}_4$ ), filtered and evaporated to yield 1.756 g (68%) of **4** as a white solid: m.p. 155–158 °C; TLC,  $R_f$  0.38 (EtOAc); ESI-MS M+Na ion calculated for  $\text{C}_{25}\text{H}_{40}\text{N}_4\text{O}_6\text{Na}$ , 515 *m/z*; found, 515.0 *m/z*;  $^1\text{H}$  NMR (300 MHz,  $\text{CDCl}_3$ ) *d* 7.40–7.30 (5H, m), 6.75 (1H, d, *J* = 7.3 Hz), 6.60 (1H, br s), 5.20–5.00 (4H, m), 4.44 (1H, m), 3.98 (1H, m), 3.20 (2H, m), 2.81 (3H, d, *J* = 3.4 Hz), 2.20–1.30 (7H, m), 1.45 (9H, s), 0.99 (3H, d, *J* = 7.3 Hz), 0.93 (3H, d, *J* = 7.3 Hz).

#### 3.4. Preparation of Boc-Ala-Val-Lys(Z)-NHMe (**5**)

A solution of 0.5168 g (1.050 mmol) of Boc-Val-Lys(Cbz)-NHMe (**4**) in 10 mL  $\text{CH}_2\text{Cl}_2$  and 1.0 mL of anisole was chilled to 5 °C in an ice water bath. To the chilled solution was added 5.0 mL TFA. The resulting solution stirred for 1.5 h while it slowly warmed to 23 °C. The solvents were evaporated to yield an oil with a red/orange color. This oil was dried under high vacuum to remove any last traces of TFA. Next, the oil was redissolved in 10 mL  $\text{CH}_2\text{Cl}_2$ . To this solution was added 0.3066 g (1.071 mmol) of Boc-Ala-OSu and 5.0 mL (30 mmol) of DIEA. The resulting solution stirred at 23 °C for 4 h. The solvent was evaporated and the residue that remained was redissolved in 200 mL  $\text{CH}_2\text{Cl}_2$  and 10 mL MeOH. This solution was washed: 3 × 200 mL 0.1 M HCl, 3 × 200 mL saturated  $\text{NaHCO}_3$ , and 1 × 200 mL brine. The organic layer was dried ( $\text{MgSO}_4$ ), filtered and evaporated to yield 0.470 g (80%) of **5** as an off-white solid: TLC,  $R_f$  0.11 (EtOAc); ESI-MS M+Na ion calculated for  $\text{C}_{28}\text{H}_{45}\text{N}_5\text{O}_7\text{Na}$ , 586 *m/z*; found, 585.8 *m/z*;  $^1\text{H}$  NMR (300 MHz,  $\text{CDCl}_3$ ) *d* 7.40–7.30 (5H, m), 6.96 (1H, m), 6.64 (2H, m), 5.10 (2H, m), 4.92 (2H, m), 4.40 (1H, m), 4.18 (1H, m), 4.06 (1H, m), 3.18 (2H, m), 2.78 (3H, d, *J* = 4.4 Hz), 2.38 (1H, m), 2.00 (1H, m), 1.90–1.20 (8H, m), 1.44 (9H, s), 0.98 (3H, d, *J* = 6.8 Hz), 0.90 (3H, d, *J* = 6.8 Hz).

#### 3.5. Preparation of Boc-Lys(Z)-Ala-Val-Lys(Z)-NHMe (**6**)

A solution of 0.988 g (1.75 mmol) of Boc-Ala-Val-Lys(Cbz)-NHMe (**5**) in 30 mL  $\text{CH}_2\text{Cl}_2$  and 1.0 mL of anisole was chilled to 5 °C in an ice water bath. To the chilled solution was added 15 mL TFA. The resulting solution stirred for 1.5 h while it slowly warmed to 23 °C. The solvents were evaporated to yield an oil with a red color. This oil was dried under high vacuum to remove any last traces of TFA. Next, the oil was redissolved in 10 mL DMF. To this solution was added 0.745 g (1.56 mmol) of Boc-Lys(Cbz)-OSu (**2**) and 6.0 mL (36 mmol) of DIEA. The resulting solution stirred at 23 °C. After 4 h the reaction solution was poured into 50 mL  $\text{CH}_2\text{Cl}_2$  and was washed: 3 × 100 mL 0.1 M HCl, 3 × 100 mL saturated  $\text{NaHCO}_3$ , and 1 × 100 mL brine. The organic layer was dried ( $\text{MgSO}_4$ ), filtered and evaporated to yield 0.968 g (67%) of **6** as an off-white solid: m.p. 185–190 °C; ESI-MS M+Na ion calculated for  $\text{C}_{42}\text{H}_{63}\text{N}_7\text{O}_{10}\text{Na}$ , 848 *m/z*; found, 847.6 *m/z*;  $^1\text{H}$  NMR (300 MHz,  $d_6$ -DMSO) *d* 8.00–7.70 (4H, m), 7.50–7.20 (12H, m), 6.92 (1H, m), 5.02 (4H, m), 4.36 (1H, m), 4.14 (2H, m), 3.87 (1H, m), 2.98 (4H, m), 2.57 (3H, d, *J* = 4.4 Hz), 1.98 (1H, m), 1.80–1.00 (15H, m), 1.44 (9H, s), 0.82 (3H, d, *J* = 7.3 Hz), 0.78 (3H, d, *J* = 6.8 Hz).

### 3.6. Preparation of metallacyclicpeptide (**1**)

A solution of 0.210 g (0.254 mmol) of **6** in 50 mL MeOH was placed in a Parr hydrogenation vessel. To this solution was added 0.102 g of 5% Pd–C. The resulting mixture was hydrogenated at 30 psi for 24 h. The catalyst was removed by vacuum filtration through celite, and the filtrate was evaporated. The solid that remained was redissolved in 100 mL anhydrous DMF and 200 mL anhydrous CH<sub>2</sub>Cl<sub>2</sub> and was placed in a flask equipped with an addition funnel. To the flask was added 0.40 mL DIEA (2.4 mmol); to the addition funnel was added a solution of 0.091 g (0.29 mmol) of 1,1'-ferrocenediacid chloride in 30 mL CH<sub>2</sub>Cl<sub>2</sub>. The solution in the addition funnel was added to the flask dropwise over 1 h. The resulting solution stirred for 18 h. Evaporation of the solvents yielded a black solid. Flash chromatography (9:1 EtOAc/MeOH) produced 0.041 g (20%) of pure **1** as an orange solid; TLC, *R*<sub>f</sub> 0.46 (9:1 EtOAc/MeOH); HPLC, *R*<sub>f</sub> 6.6 min; ESI-MS M+Na ion calculated for C<sub>38</sub>H<sub>57</sub>N<sub>7</sub>O<sub>8</sub>FeNa, 818 *m/z*; found, 818.0 *m/z*; HRMS M+H ion calculated for C<sub>38</sub>H<sub>58</sub>N<sub>7</sub>O<sub>8</sub>Fe, 796.369705 *m/z*; found, 796.369385 *m/z*; <sup>1</sup>H NMR (400 MHz, CDCl<sub>3</sub>) *d* 8.02 (1H, m), 7.31 (1H, d, *J* = 7.5 Hz), 7.10 (1H, d, *J* = 6.2 Hz), 6.92 (1H, m), 6.58 (1H, d, *J* = 3.3 Hz), 6.25 (1H, t, *J* = 5.6 Hz), 5.31 (1H, d, *J* = 2.8 Hz), 4.54–4.32 (8H, m), 4.20 (1H, m), 4.14 (2H, m), 3.96 (1H, m), 3.60 (1H, m), 3.52 (1H, m), 3.32 (1H, m), 3.17 (1H, m), 2.80 (3H, d, *J* = 4.6 Hz), 2.42 (1H, m), 2.20–1.35 (12H, m), 1.47 (9H, s), 1.27 (3H, d, *J* = 1.6 Hz), 1.05 (6H, d, *J* = 7.0 Hz).

### Acknowledgements

This work was supported by summer undergraduate research fellowships to ELH by Pfizer and the Connecticut Business and Industry Association (CBIA), and by Bristol-Myers Squibb. This work was also supported by an NSF-MRI Award (CHE-0619275) for the NMR spectrometer used in these experiments. We thank JEOL for their assistance in obtaining a high-resolution mass spectrum of **1**; Whitney Smith, Jon Weiss, Andrew Rosenau, Neena Chakrabarti, Peter Hendrickson and Julianne Boccuzzi for their assistance in obtaining routine <sup>1</sup>H NMR spectra; and Professor Richard Prigodich (Trinity College) for his assistance obtaining the CD spectrum. Finally, we thank the Trinity College Faculty Research Committee for financial support.

### Appendix A. Supplementary material

Supplementary data associated with this article can be found, in the online version, at doi:10.1016/j.jorganchem.2008.11.055.

### References

- [1] T.E. Creighton, *Proteins Structures and Molecular Properties*, W.H. Freeman and Company, New York, 1993.
- [2] R. Lavery, *Q. Rev. Biophys.* 38 (2005) 339–344.

- [3] A. Klug, *FEBS Lett.* 579 (2005) 892–894.
- [4] M. Sattler, H. Liang, D. Nettlesheim, R.P. Meadows, J.E. Harlan, M. Eberstadt, H.S. Yoon, S.B. Shuker, B.S. Chang, A.J. Minn, C.B. Thompson, S.W. Fesik, *Science* 275 (1997) 983–986.
- [5] X. Liu, S. Dai, Y. Zhu, P. Marrack, J.W. Kappler, *Immunity* 19 (2003) 341–352.
- [6] L.D. Walensky, A.L. Kung, I. Escher, T.J. Malia, S. Barbuto, R.D. Wright, G. Wagner, G.L. Verdine, S.J. Korsmeyer, *Science* 305 (2004) 1466–1470.
- [7] M.J. Kelso, D.P. Fairlie, *Molecular pathomechanisms and new trends*, in: G. Keri, I. Toth (Eds.), *Drug Research*, Taylor and Francis, London, 2003, pp. 578–598.
- [8] D.S. Kemp, *Trend. Biotechnol.* 8 (1990) 249–255.
- [9] J.P. Schneider, J.W. Kelly, *Chem. Rev.* 95 (1995) 2169–2187.
- [10] M.J.J. Andrews, A.B. Tabor, *Tetrahedron* 55 (1999) 11711–11743.
- [11] J. Garner, M.M. Harding, *Org. Biomol. Chem.* 5 (2007) 3577–3585.
- [12] D.S. Kemp, T.P. Curran, J.G. Boyd, T.J. Allen, *J. Org. Chem.* 56 (1991) 6683–6697.
- [13] G.E. Job, R.J. Kennedy, B. Heitmann, J.S. Miller, S.M. Walker, D.S. Kemp, *J. Am. Chem. Soc.* 128 (2006) 8227–8233.
- [14] R.E. Austin, R.A. Maplestone, A.M. Sefler, K. Liu, W.N. Hruzewicz, C.W. Liu, H.S. Cho, D.E. Wemmer, P.A. Bartlett, *J. Am. Chem. Soc.* 119 (1997) 6471–6472.
- [15] N.E. Shepherd, H.N. Hoang, V.S. Desai, E. Letouze, P.R. Young, D.P. Fairlie, *J. Am. Chem. Soc.* 128 (2006) 13284–13289.
- [16] A.K. Galande, K.S. Bramlett, J.O. Trent, T.P. Burris, J.L. Wittliff, A.F. Spatola, *Chembiochem* 6 (2005) 1991–1998.
- [17] M. Matzapetakis, V.L. Pecoraro, *J. Am. Chem. Soc.* 127 (2005) 18229–18233.
- [18] R.L. Beyer, H.N. Hoang, T.G. Appleton, D.P. Fairlie, *J. Am. Chem. Soc.* 126 (2004) 15096–15105.
- [19] J.A. Ihalainen, J. Bredenbeck, R. Pfister, J. Helbing, L. Chi, I.H. van Stokkum, G.A. Woolley, P. Hamm, *Proc. Natl. Acad. Sci. USA* 104 (2007) 5383–5388.
- [20] D. Wang, K. Chen, G. Dimartino, P.S. Arora, *Org. Biomol. Chem.* 4 (2006) 4074–4081.
- [21] S. Kirin, H.-B. Kraatz, N. Metzler-Nolte, *Chem. Soc. Rev.* 35 (2006) 348–354.
- [22] D.R. van Staveren, N. Metzler-Nolte, *Chem. Rev.* 104 (2004) 5931–5985.
- [23] S. Chowdhury, K.A. Mahmoud, G. Schatte, H.-B. Kraatz, *Org. Biomol. Chem.* 3 (2005) 3018–3023.
- [24] S.I. Kirin, U. Schatzschneider, X. de Hatten, T. Weyhermüller, N. Metzler-Nolte, *J. Organomet. Chem.* 691 (2004) 3451–3457.
- [25] T. Moriuchi, T. Nagai, T. Hirao, *Org. Lett.* 8 (2006) 31–34.
- [26] T. Moriuchi, A. Nomoto, K. Yoshida, A. Ogawa, T. Hirao, *J. Am. Chem. Soc.* 123 (2001) 68–75.
- [27] R.S. Herrick, R.M. Jarret, T.P. Curran, D.R. Dragoli, M.B. Flaherty, S.E. Lindyberg, R.A. Slate, *Tetrahedron Lett.* 37 (1996) 5289–5292.
- [28] M. Pellegrini, M. Royo, M. Chorev, D.F. Mierke, *J. Pept. Res.* 49 (1997) 404–414.
- [29] W. Zhang, J.W. Taylor, *Tetrahedron Lett.* 37 (1996) 2173–2176.
- [30] E. Schievano, A. Bisello, M. Chorev, A. Bisol, S. Mammi, E. Peggion, *J. Am. Chem. Soc.* 123 (2001) 2743–2751.
- [31] A.K. Boal, I. Guryanov, A. Moretto, M. Crisma, E.L. Lanni, C. Toniolo, R.H. Grubbs, D.J. O'Leary, *J. Am. Chem. Soc.* 129 (2007) 6986–6987.
- [32] E.W. Knobloch, W.H. Rauscher, *J. Polym. Sci.* 54 (1961) 651–656.
- [33] N. Greenfield, G.D. Fasman, *Biochemistry* 8 (1969) 4108–4116.
- [34] A. Pardi, M. Billeter, K. Wuthrich, *J. Mol. Biol.* 180 (1984) 741–751.
- [35] V.F. Bystron, *Prog. NMR Spectrosc.* 10 (1976) 41–82.
- [36] C. Toniolo, E. Benedetti, *Trend. Biochem. Sci.* 16 (1991) 350–353.
- [37] D.J. Barlow, J.M. Thornton, *J. Mol. Biol.* 201 (1984) 601–619.
- [38] S. Hanessian, G. Papeo, K. Fettes, E. Therrien, M.T.P. Viet, *J. Org. Chem.* 69 (2004) 4891–4899.
- [39] S.K. Maji, D. Haldar, D. Bhattacharyya, A. Bannerjee, *J. Mol. Struct.* 646 (2003) 111–123.
- [40] S. Vijayalakshmi, R.B. Rao, I.L. Karle, P. Balaram, *Biopolymers* 53 (2000) 84–98.
- [41] R.M. Jain, K.R. Rajashankar, S. Ramakumar, V.S. Cahuhan, *J. Am. Chem. Soc.* 119 (1997) 3205–3211.
- [42] I.L. Karle, A. Pramanik, A. Bannerjee, S. Bhattacharyya, P. Balaram, *J. Am. Chem. Soc.* 119 (1997) 9087–9095.
- [43] T.P. Curran, K.A. Marques, M.V. Silva, *Org. Biomol. Chem.* 3 (2005) 4134–4138.